TISSUE ENGINEERING: Part A
Volume 15, Number 8, 2009

DOI: 10.1089/ten.tea.2008.0305

Original Article

Basic Fibroblast Growth Factor Delivery Enhances Adrenal Cortical Cellular Regeneration

Yinting Chu, Ph.D.,[1] Won Jin Ho, B.S.,[1] and James C.Y. Dunn, M.D., Ph.D.[1,2]

The effective delivery of angiogenic factors is a useful strategy for the engineering of vascularized tissues. When adrenal cortical cells were implanted in mice under the renal capsule, the size of the implant was reduced to about 100 μm in thickness after 8 weeks. Either low (~2 μg) levels of basic fibroblast growth factor (bFGF) or high (~12 μg) levels of bFGF were encapsulated into poly-lactic-*co*-glycolic acid microspheres, and these bFGF-encapsulated microspheres were coimplanted with adrenal cortical cells. After 56 days, the implants with low and high levels of bFGF weighed five and eight times more, respectively, than the implants without bFGF delivery. The implants with bFGF-encapsulated microspheres also contained significantly more cells than the implants without bFGF delivery. The levels of adrenal cortical gene expression were not significantly changed with bFGF delivery. The implants with high levels of bFGF also had a more uniform distribution of anti-CD31 immunofluorescence. Based on the increased number of cells that expressed adrenal cortical genes, the delivery of bFGF enhanced adrenal cortical cellular regeneration, possibly through an angiogenic response.

Introduction

The adrenal cortex secretes essential hormones, such as cortisol and aldosterone, that are critical to homeostasis. The destruction of the adrenal cortex due to autoimmune diseases and tuberculosis can lead to adrenal insufficiency. The current treatment for adrenal insufficiency is hormonal replacement therapy in which patients receive daily supplemental corticosteroids.[1] However, because excessive hormonal replacement can lead to undesired side effects, including osteoporosis, weight gain, and high blood pressure, it is ideal to provide the patients with only the minimum dosage that relieves their symptoms.[2] The inability of the hormonal replacement to meet physiological demands due to stress poses a serious health problem. Previous research has shown that transplanted adrenal cortical cells could regenerate adrenal tissues and represent a potential approach in the treatment of adrenal insufficiency.[3,4] The regenerated adrenal tissues could respond appropriately to varying physiological demands.

Previously, we found that implanted adrenal cells sustained the expression of adrenal cortical genes, but the size of the tissue construct diminished significantly after 8 weeks.[3] Because the overall function of the tissue depends on the function of the cells as well as the number of functional cells, the growth and survival of the implanted adrenal cortical cells are critical to the success of such cell-based therapy. Adrenal cortical cells are mitogenically stimulated by both basic and acidic fibroblast growth factor (bFGF and aFGF, respectively).[5,6] The expression of bFGF and its receptors in the adrenal cortex are regulated by adrenocorticotropic hormone.[6–9] bFGF is also one of the key angiogenic factors. It induces endothelial cell replication, migration, and extracellular proteolysis.[10–12] Its activity has been evaluated in different *in vitro* as well as *in vivo* experimental models. Pepper *et al*. have demonstrated that bFGF induces angiogenesis *in vitro* via direct effects on endothelial cells.[13] Further, using epidermoid lung carcinoma samples from 84 patients, Mattern *et al*. showed that expression of bFGF *in vivo* is highly correlated with vessel density.[14] bFGF may promote angiogenesis both by directly acting on endothelial cells and by indirectly upregulating the expression of vascular endothelial growth factor in endothelial cells.[15]

The delivery of growth factors can be achieved using DNA or proteins. Plasmid DNA can be directly introduced to express growth factors.[16] Alternatively, growth factor genes can be delivered via viral vectors[17] or genetically modified cell lines.[18,19] More directly, growth factors can be delivered at the protein level. The controlled release of growth factors can promote tissue development and formation.[20] A common method by which growth factors have been delivered is encapsulation within microspheres.[21,22] Poly(lactic-*co*-glycolic acid) (PLGA) has been employed in a number of devices approved for use by the Food and Drug Administration.[23,24] PLGA degrades by hydrolysis to lactic and glycolic acid, and it

[1]Biomedical Engineering Interdepartmental Program, Department of Bioengineering, University of California–Los Angeles, Los Angeles, California.
[2]Department of Surgery, University of California–Los Angeles, Los Angeles, California.

is also easily processed, making it attractive for the fabrication of microspheres with adjustable degradation rates.[24] In this study, we stimulated implanted adrenal cortical cell seeded on collagen sponges by utilizing bFGF-encapsulated PLGA microspheres. We hypothesized that bFGF will improve the growth of the implants and will regulate the gene expression of adrenal cortical cells within the implants.

Materials and Methods

Materials

Dulbecco's modified Eagle's medium and Ham's F12 medium (DMEM/F12), phosphate-buffered saline (PBS), Hank's balanced salt solution (HBSS), fetal bovine serum (FBS), horse serum, and antibiotic–antimycotic solution containing penicillin, streptomycin, and amphotericin B were purchased from Invitrogen (Carlsbad, CA). Ethanol, acetone, Tris-buffered saline, Tween 20, collagenase I, deoxyribonuclease I, bovine serum albumin (BSA), Trypan Blue, polyvinyl alcohol (PVA) (87–89% hydrolyzed, Mw 31,000–50,000) and polyvinyl pyrolidone (PVP) (Mw 10,000), chloroform, and methanol were purchased from Sigma–Aldrich (St. Louis, MO). Helistat collagen sponge was purchased from Integra LifeSciences (Plainsboro, NJ). PLGA (lactide:glycolide ratio 85:15, intrinsic viscosity 0.61 dL/g) was purchased from Birmingham Polymers (Birmingham, AL). Type I collagen solution purified from bovine skin was obtained from Vitrogen (Palo Alto, CA). Recombinant human bFGF was provided by the National Institutes of Health. SeaPlaque Agarose was purchased from Lonza (Rockland, ME). GAPDH primers and probe were purchased from Applied Biosystems (Foster City, CA).

Animals

Eight-week-old female C57/BL mice were purchased from the Jackson Laboratory (Bar Harbor, ME). All animals were maintained and handled in compliance with the institutional regulations established and approved by the Animal Research Committee at the University of California, Los Angeles. Mice were housed in cages under standard laboratory conditions.

Encapsulation of bFGF into PLGA microspheres

bFGF-encapsulated PLGA microspheres were prepared by the double emulsion solvent evaporation method.[25–27] A sonicator with a microtip (Sonic Dismembrator 500; Fisher Scientific, Hampton, NH) was used to emulsify 100 μL of protein solution containing 10 or 90 μg of bFGF (the low and high bFGF groups), or no bFGF as the control group, in PBS with 0.1% BSA and 500 μL of 0.5% (w/w) solution of PLGA in chloroform for 1 min on ice to produce the primary emulsion. The concentration of bFGF in the initial protein solution was provided by the company. A water–oil–water emulsion was then created by emulsifying the primary emulsion with 2 mL of 2% (w/v) PVA solution using the same sonicator for 1 min on ice. Subsequently, the resulting double emulsion was transferred into 40 mL of 0.5% (w/v) PVA/PVP solution and was magnetically stirred at room temperature for 20 h to evaporate the solvent. The microspheres were collected by centrifugation at 4500 *g* for 30 min at 4°C and were washed three times with distilled water. The washed microspheres were then divided into three equal aliquots for three implants.

Integrity of encapsulated bFGF and efficiency of bFGF encapsulation

The integrity of encapsulated bFGF was evaluated by Western blotting.[27] One aliquot of microspheres used for one implant from each groups was freeze-dried and dissolved in 1 mL of chloroform/acetone (1:1 ratio). The solution was vortexed and centrifuged at 8000 *g*, and the resulting pellet was washed with chloroform/acetone two more times. After the evaporation of organic solvents, the pellet was dissolved in 100 μL of PBS. About 2.5 μL of the protein samples were mixed with 27.5 μL of PBS containing 25% reducing sample buffer (Thermo Scientific, Rockford, IL), heated at 95°C for 10 min, and subsequently resolved by SDS-PAGE (15%; Bio-Rad, Hercules, CA) and transferred to PVDF membranes (0.2 μm; Bio-Rad). Free bFGF (100, 400, and 600 ng) served as standards to determine the amount of encapsulated bFGF. The membranes were blocked with 5% skim milk (Bio-Rad) in Tris-buffered saline containing 0.1% Tween 20 (TBST) and 1% horse serum for 1 h at room temperature, which was followed by 1-h incubation at room temperature with rabbit anti-bFGF antibodies (R&D Systems, Minneapolis, MN) (1:2000). After washing with TBST, the membranes were incubated with horseradish peroxidase–conjugated anti-rabbit IgG (BD Biosciences, San Jose, CA) for 1 h at room temperature (1:5000, all dilutions in 5% skim milk in TBST). After washing with TBST, blots were visualized by chemiluminescence (ECL kit; Pierce, Rockford, IL). Images of the blots were taken using the LAS-3000 Image Reader (Fujifilm, Cypress, CA), and images were analyzed using the Multi Gauge software (Fujifilm). The content, recovery, and encapsulation of bFGF were calculated as follows:

$$\text{Theoretical bFGF content} = \frac{\text{mass of bFGF used in the formulation}}{\text{mass of PLGA and bFGF used in the formulation}}$$

$$\text{Microsphere recovery} = \frac{\text{mass of microspheres recovered}}{\text{mass of PLGA and bFGF used in the formulation}}$$

$$\text{Actual bFGF content} = \frac{\text{mass of bFGF in microspheres}}{\text{mass of microspheres recovered}}$$

$$\text{bFGF encapsulation efficiency} = \frac{\text{mass of bFGF in microspheres}}{\text{mass of bFGF used in the formulation}}$$

Isolation of adrenal cells

For each preparation, 10 murine adrenal glands were removed from animals after euthanasia.[28] After removing the surrounding fat, they were incubated in the digestion mixture at 37°C for 1 h with gentle shaking. The digestion

mixture consisted of 10 mL of HBSS containing 2 mg/mL collagenase I, 0.05 mg/mL DNase I, and 5 mg/mL BSA.[3] After dispersing the cells through a pipette, they were washed and filtered through a 40-μm strainer (Millipore, Bedford, MA) and were counted with a hemacytometer. The viability was assessed by Trypan Blue exclusion.

Implantation

Approximately one million cells were resuspended in 30 μL of sera-containing medium, composed of DMEM/F12 with 15% heat-inactivated horse serum, 2.5% heat-inactivated FBS, 100 U/mL penicillin, 100 μg/mL streptomycin, and 250 ng/mL amphotericin B,[28] containing 0.24 mg/mL of neutralized collagen and microspheres before seeding onto a collagen sponge that was 3×2×7 mm in size. Neutralized collagen was made by mixing 80 μL of collagen with 10 μL of 10× PBS and 10 μL of 0.1N sodium hydroxide solution. The cell-seeded collagen sponges were then placed in the incubator to allow the cells to attach for an hour before implantation. The final cell and PLGA microsphere concentrations in the implants were approximately 24,000 cells/μL and 30 mg/mL, respectively. Female recipient mice were anesthetized with 5% isoflurane and 1 L/min oxygen for 2 min. The dorsal skin was prepared neck through tail with three alternative scrubs of 10% betadine (Purdue, Stamford, CT) and 70% ethanol. Mice were positioned prone under maintenance of general anesthesia through inhaling combination of 2.5% isoflurane and 0.5 L/min oxygen. A 3-cm incision was made through dorsal midline. The subcutaneous tissue was detached bluntly. Myotomy of the right flank was performed parallel to the lower edge of the liver. The left adrenal gland was identified within the space defined by the hepatic lower edge, the renal upper pole, and the spinal column. The adrenal pedicle was clamped tightly for 5 s before adrenalectomy. The kidney was exteriorized without tension and temporarily fixed with moist gauze. The ventral renal capsule was lifted away from the renal cortex through a transverse incision. The implant was inserted under the renal capsule. The kidney was returned without torsion of the renal pedicle. Muscular layers were closed with 6–0 Prolene sutures (Ethicon, Piscataway, NJ), and the skin was sutured with 3–0 Vicryl (Ethicon, Piscataway, NJ). Mice were euthanized through inhalational isoflurane at 10, 28, and 56 days. At the time of harvest, the implants were clearly distinguishable from their sites of implantation and were excised completely with a scalpel. For histological evaluation, the specimens were fixed in formalin and were embedded in paraffin. Tissue sections were stained with hematoxylin and eosin.

RNA extraction and qRT-PCR

RNA extraction and quantitative reverse transcriptase polymerase chain reaction (qRT-PCR) was done as previously described.[28] Briefly, total RNA isolation was performed following Qiagen RNeasy Mini Kit protocols, and expressions of specific mRNAs was analyzed by qRT-PCR. *Sf1* was amplified by primers 5′-TGCTGGTGTTGGACCACATCTA-3′ and 5′-CAGTAACCAGCAGGATGCTGTCT-3′, and probe 5′-CGCC AGGTCCAGTACGGCAAGG-3′. *Cyp11b1* was amplified by 5′-AGAGCTGGCAGAGGGTCGT-3′ and 5′-TGGCATCCATT GACAGAGTTCT-3′, and probe 5′-CACAGTCCTGGAGT GTCACAGCAGAGCT-3′. *Cy11b2* was amplified by 5′-CAGA CTCGGCAGCTCTCAGA-3′ and 5′-ATGGCGTCGAGAGGC AAA-3′, and probe 5′-CTACAGTGGCATTGTGGCGGAAC TAATATCTCA-3′. *Cyp11a1* was amplified by 5′-CAACA AGCTGCCCTTCAAGAAC-3′ and 5′-ACCGTGCCACCCCT CCT-3′, and probe 5′-CCAGGCCAACATTACCGAGATGCT GT-3′. To compare *Sf1* expression over time, the relative level of *Sf1* expression was normalized to that of pooled neonatal adrenal glands. To compare gene expression between groups, the relative level of each adrenal-specific gene was normalized to that of the control group at each time point.

Immunofluorescence of CD31

Implants were retrieved and stained with anti-CD31 antibody.[29–31] Briefly, retrieved implants were fixed in 10% buffered formalin (Fisher Scientific) for 20 h at 4°C and then washed with PBS three times. Serial sections (200 μm) were cut on a Leica VT1000E Vibratome (Ted Pella, Redding, CA) through the implants. Sections were incubated with a blocking buffer of PBS containing 5% goat serum (Jackson Immunoresearch, Westgrove, PA) and 0.3% Triton for 2 h at room temperature. Rat anti-mouse CD31 antibody (Pharmingen, CA) was diluted 1:500 in the blocking buffer. The anti-CD31 antibody was detected with Cy3-labeled goat secondary anti-rat IgG antibody (Jackson Immunoresearch). Immunofluorescence was visualized on a Zeiss Axioskop microscope (Thornwood, New York). The red fluorescence intensity and the area of the scaffold in pixels were measured using the BioQuant Nova software (BioQuant Life Sciences, Nashville, TN). The blood vessel density was calculated by dividing the total intensity of the red fluorescence by the number of pixels.

Cell number determination

The number of cells in the implants was quantified by the CyQUANT Cell Proliferation Assay Kit purchased from Invitrogen following the manufacturer's protocol. Briefly, the total DNA from each implant was purified by the DNeasy Blood & Tissue Kit purchased from Qiagen (Valencia, CA). The DNA aliquots were then incubated for 5 min with the CyQUANT® GR before transferred to a 96-well microplate. The mixture was placed into a microplate reader to be read at 480 nm excitation and 520 nm emission along with a standard curve produced by serially diluted concentrations of bacteriophage λ DNA (Invitrogen) and adrenal cortical cells. The resulting fluorescence values were converted into cell numbers by referencing the standard curve.

Statistical analysis

The cell number, implant weights, anti-CD31 density, and gene expression at each time point were analyzed using ANOVA (General Linear Models, SAS/STAT; SAS Institute, Cary, NC). For measurements in which there was a significant difference, the *post hoc* testing of pairwise differences between cell groups at each time point was performed using the Tukey's Studentized Range (HSD) test (SAS/STAT). A probability of $p < 0.05$ was considered to be significant.

Results

The integrity of bFGF encapsulated within microspheres was confirmed by Western blot. Proteins extracted from the bFGF-encapsulated microspheres exhibited a dominant band

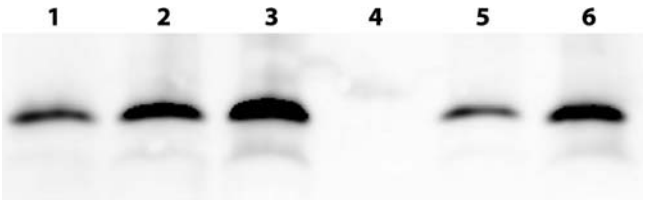

FIG. 1. Western blot analysis of bFGF extracted from PLGA microspheres. Lanes 1, 2, and 3: 100, 400, and 600 ng of bFGF, respectively; lanes 4, 5, and 6: bFGF extracted from the control, the low, and the high bFGF groups, respectively.

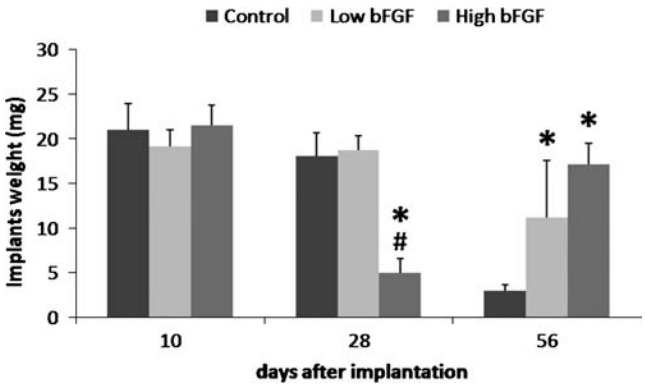

FIG. 2. Weights of retrieved implants at different time points. Implants were retrieved on days 10, 28, and 56. The weight of the high bFGF group was compared to that of the control and low bFGF groups. The weight of the low bFGF group was compared to that of the control group. $^{*}p < 0.05$ as compared to the control group, and $^{\#}p < 0.05$ as compared to the low bFGF group. Error bar represents standard deviation of measurements of retrieved implants from three animals.

with a molecular weight between 15 and 20 kDa, which was identical to the nonencapsulated bFGF (Fig. 1). Minor bands were observed, but they were also observed with the nonencapsulated bFGF. The encapsulation efficiencies were 69% for the low bFGF group and 42% for the high bFGF group (Table 1). bFGF release kinetics from similar PLGA microspheres has been previously studied *in vitro*. Despite a burst release within the first hour, bFGF delivery was maintained over a period of 30 days.[32]

Adrenal cells were seeded on collagen sponges coated with bFGF-encapsulated microspheres for implantation studies. Microscopic imaging of sections of cell-seeded scaffolds showed uniform distribution of cells within the scaffolds (data not shown). The implants appeared pale yellow at specimen retrieval. No significant differences in weight of the implants were noted after 10 days (Fig. 2). After 28 days, implants in the control and low bFGF group remained unchanged in size, but implants in the high bFGF group became smaller and weighed significantly less. After 56 days, implants in the control group decreased significantly in size, weighing only 23% of their day 10 weight. Implants in the low bFGF group also decreased their weight to 62% of their day 10 weight. In contrast, implants in the high bFGF group nearly regained their day 10 weight after 56 days.

Histologically, the implants appeared as sponge-like structures, and cells were distributed throughout the implants in all three groups after 10 days (Fig. 3). These sponge-like structures were still observed in the control and the low bFGF group after 28 days. In the control group, central areas devoid of cells were observed. This was less prominent in the low bFGF group, where a denser cell distribution was observed. After 28 days, less void space was observed in the high bFGF group, and there was a more uniform cell distribution than the other groups. After 56 days, the sponge-like structures were not observed in any of the groups, and cells distributed much more uniformly than they were on day 10 or 28. Vascular structures of capillaries containing red blood cells could be identified in the micrographs under higher magnification (data not shown). The implants in the control group diminished to about 100 μm in thickness by day 56, whereas the low and high bFGF groups had larger-size implants with organized tissues.

After 10 days of implantation, the low and high bFGF groups had similar number of cells, and both had significantly more cells than the control group (Fig. 4). The cell number in the control and the low bFGF groups increased overtime after day 10. In contrast, after 28 days, the high bFGF group had the least cells but increased drastically by day 56.

Blood vessel ingrowth into the implants was visualized by anti-CD31 immunofluorescence (Fig. 5) Blood vessel ingrowth was observed 10 days after the implantation in all groups. On day 10, both the low and the high bFGF groups had stronger anti-CD31 staining on the periphery of the implants than the control group. On day 28, central areas without anti-CD31 staining were observed in the control and the low bFGF group (Fig. 5D, E), similar to the voids observed in the histological sections (Fig. 3D, E). In the high bFGF group, a uniform anti-CD31 was observed in the implants, even though the overall size was significantly smaller. On day 56, all three groups showed a more uniform distribution of anti-CD31 staining than on day 28. The high bFGF group had higher blood vessel density than the control group at all time points, and it was also higher than the low bFGF group on days 28 and 56 (Fig. 6).

The expression of *Sf1* in the control group decreased over the first 28 days, but increased after 56 days of implantation (Fig. 7). The low and high bFGF groups followed similar

Table 1. Characterization of bFGF-Encapsulated PLGA Microspheres Prepared with the Double Emulsion Method

Group	*Theoretical bFGF content (%)*	*Microsphere recovery (%)*	*Actual bFGF content (%)*	*bFGF encapsulation efficiency (%)*	*bFGF delivered per scaffold (μg)*
Control	0	89	—	—	0
Low	0.27	84	0.22	69	2.3
High	2.43	81	1.25	42	12.5

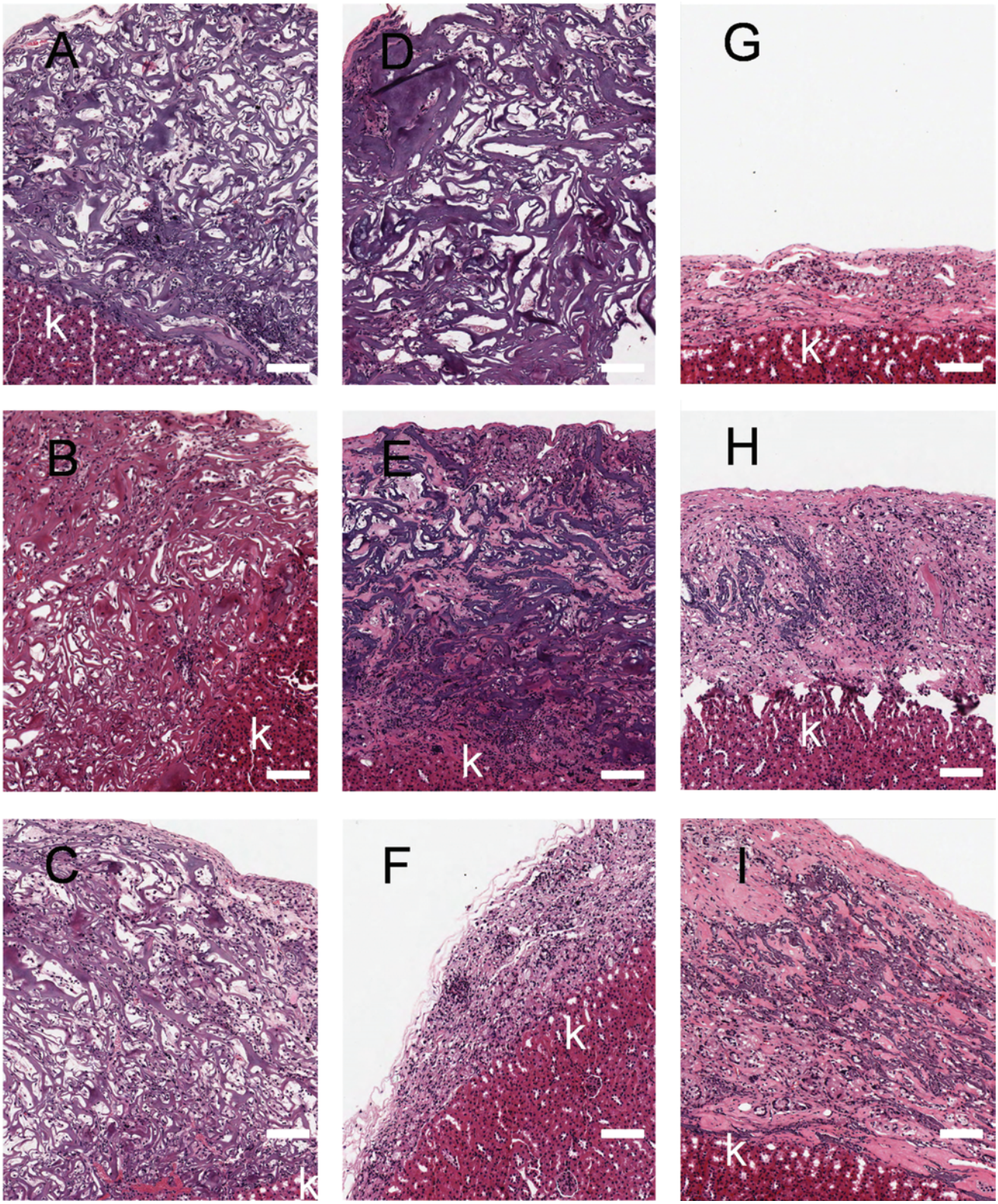

FIG. 3. Histological appearance of tissues formed from the implanted adrenal cortical cells and bFGF delivery. Hematoxylin/eosin stain, 100×. (**A**), (**B**), and (**C**) were retrieved on day 10; (**D**), (**E**), and (**F**) were retrieved on day 28; (**G**), (**H**), and (**I**) were retrieved on day 56. (**A**), (**D**), and (**G**) are from the control group; (**B**), (**E**), and (**H**) are from the low bFGF group; (**C**), (**F**), and (**I**) are from the high bFGF group. Scale bar, 100 μm. k, kidney. The micrographs are representative of results from three experiments. Color images available online at www.liebertonline.com/ten.

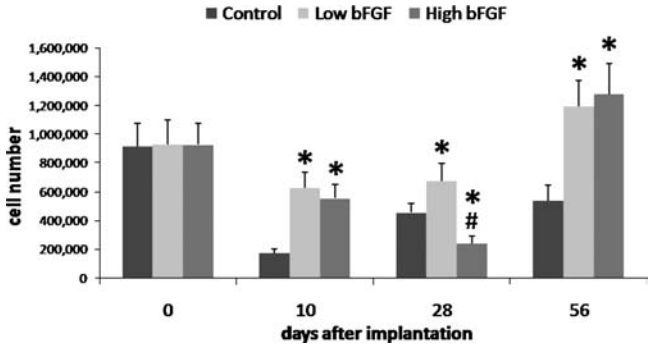

FIG. 4. Average cell numbers within the retrieved implants. Implants were retrieved on days 10, 28, and 56. The cell number of the high bFGF group was compared to that of the control and low bFGF groups. The cell number of the low bFGF group was compared to that of the control group. $^{*}p < 0.05$ as compared to the control group, and $^{\#}p < 0.05$ as compared to the low bFGF group. Error bar represents standard deviation of measurements of retrieved implants from three animals.

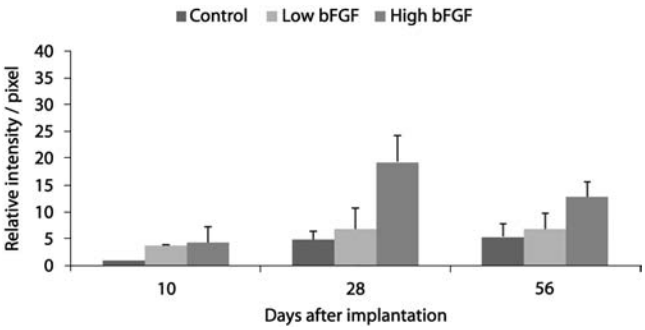

FIG. 6. Relative intensity of anti-CD31 staining per area of implants. Images of implants retrieved on days 10, 28, and 56 were analyzed as described in Materials and Methods section. Relative intensity per pixel of each group was calculated by normalizing to that of the control group on day 10. The values are means ± standard deviation of measurements from two experiments.

trend. When compared between groups, both the low and high bFGF groups expressed similar levels of adrenal cortical genes as the control group initially and on day 10 (Fig. 8). On days 28 and 56, the control group and the low bFGF group had similar gene expression profile. Implants in the high bFGF group had statistically significantly higher level of *Cyp11b2* and *Cyp11a1* gene expression than implants in the control group on day 28. On day 56, the implants in the high bFGF group had higher level of *Cyp11b2* gene expression than the implants in both the control group and the low bFGF group.

Discussion

Previously, we reported the successful implantation of adrenal cortical cells under the renal capsule.[3] The expression of adrenal-specific markers, including *Sf1, Dax1, Cyp11a1, Cyp11b1,* and *Cyp11b2,* was detectable in the retrieved specimens over a period of 8 weeks postimplantation. In scaffolds that were implanted without cells, no adrenal-specific markers could be detected. While these results were encouraging, the size of the retrieved implants was reduced to about 100 μm thick. The number of cells surviving the implantation process is critical because sufficient amount of steroid hormones needs to be secreted by the adrenal cells to affect physiological functions. Ideally, the cells not only survive but also grow at the implantation site. Vascularization of the implant is crucial because it affects the transport of nutrients, waste products, as well as hormones in the environment. Stimulation of blood vessel ingrowth into the implants may improve angiogenesis and support the survival and growth of the adrenal cortical cells. Numerous strategies have been used to stimulate blood vessel ingrowth within the implant sites. Among them, the most potent method is to deliver angiogenic growth factors such as vascular endothelial growth factor or bFGF.[33] These growth factors are normally secreted by wound-healing cells such as macrophages. bFGF was chosen in this study because not only does

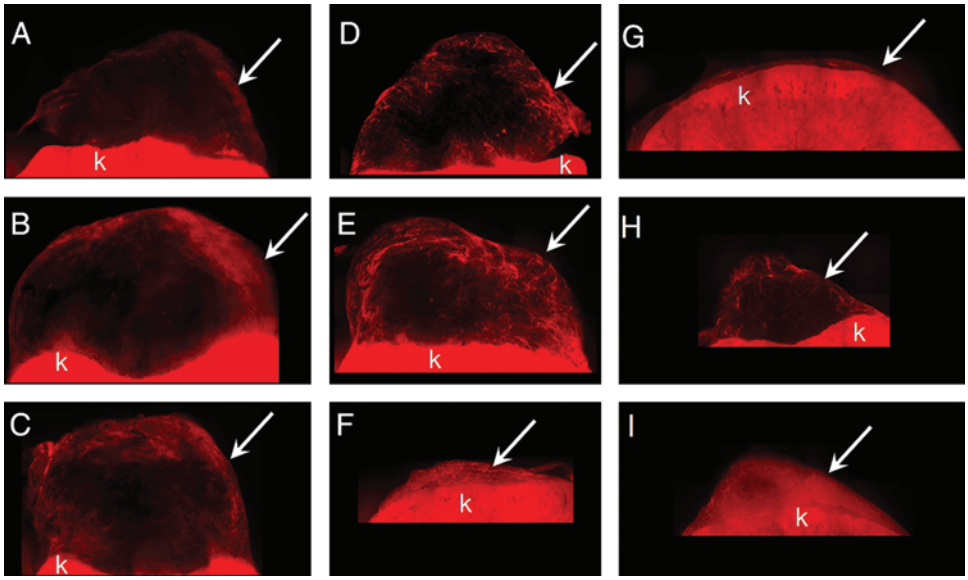

FIG. 5. Immunofluorescence of anti-CD31 staining. (**A**), (**B**), and (**C**) were retrieved on day 10; (**D**), (**E**), and (**F**) were retrieved on day 28; (**G**), (**H**), and (**I**) were retrieved on day 56. (**A**), (**D**), and (**G**) are from the control group; (**B**), (**E**), and (**H**) are from the low bFGF group; (**C**), (**F**), and (**I**) are from the high bFGF group. Arrows indicate location of the implants. k, kidney. Color images available online at www.liebertonline.com/ten.

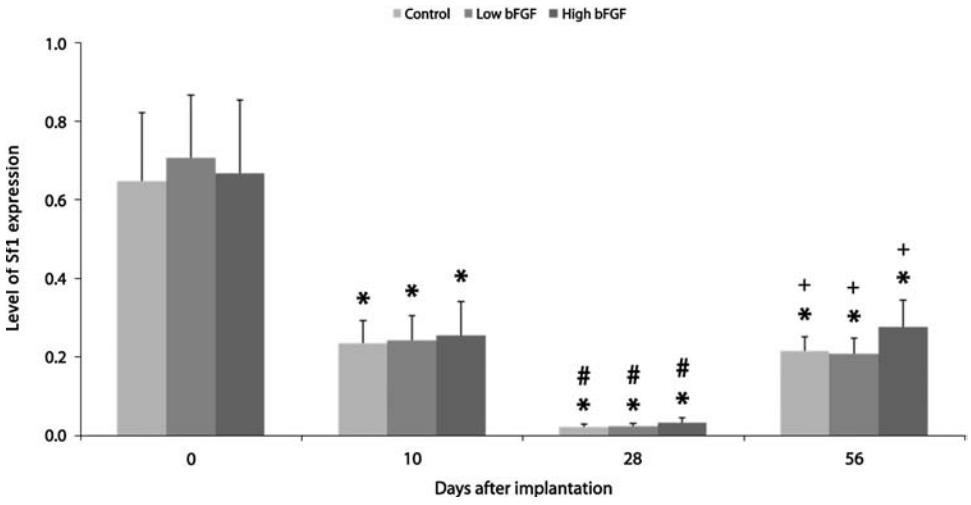

FIG. 7. *Sf1* gene expression in the control, low bFGF, and high bFGF group. Expression level was normalized to pooled neonatal adrenal glands. The gene expression level of implants retrieved at later time points was compared to that of earlier time points. $^{*}p < 0.05$ as compared to the day 0; $^{\#}p < 0.05$ as compared to day 10; $^{+}p < 0.05$ as compared to day 28. Error bar represents standard deviation of measurements of retrieved implants from three animals.

it stimulate angiogenesis, but it also affects the function of adrenal cortical cells, both *in vivo* and *in vitro*.[6,8,9,18,34]

To promote adrenal cell growth and vascular system formation, genetically modified 3T3 cells that produce aFGF were cotransplanted with adrenal cortical cells in severe combined immunodeficient mice. The results from these studies demonstrated increased angiogenesis at the implant sites.[18,35,36] In the groups without aFGF delivery, necrotic centers were observed, and the function of the transplanted tissue was hindered.[18,35,36] In our study, a polymer-based system was selected because a controlled amount of bFGF could be delivered. These microspheres were previously shown to support the growth of smooth muscle cells *in vivo* for up to 28 days.[21] The delivery of bFGF by microspheres was more effective than the delivery of bFGF-incorporated collagen. Western blot results showed that encapsulated bFGF was not altered in size during the preparation of microspheres.

The most striking finding was the significant size reduction in the high bFGF group on day 28. As expected, the angiogenic response correlated with the dose of bFGF, but the size and cell

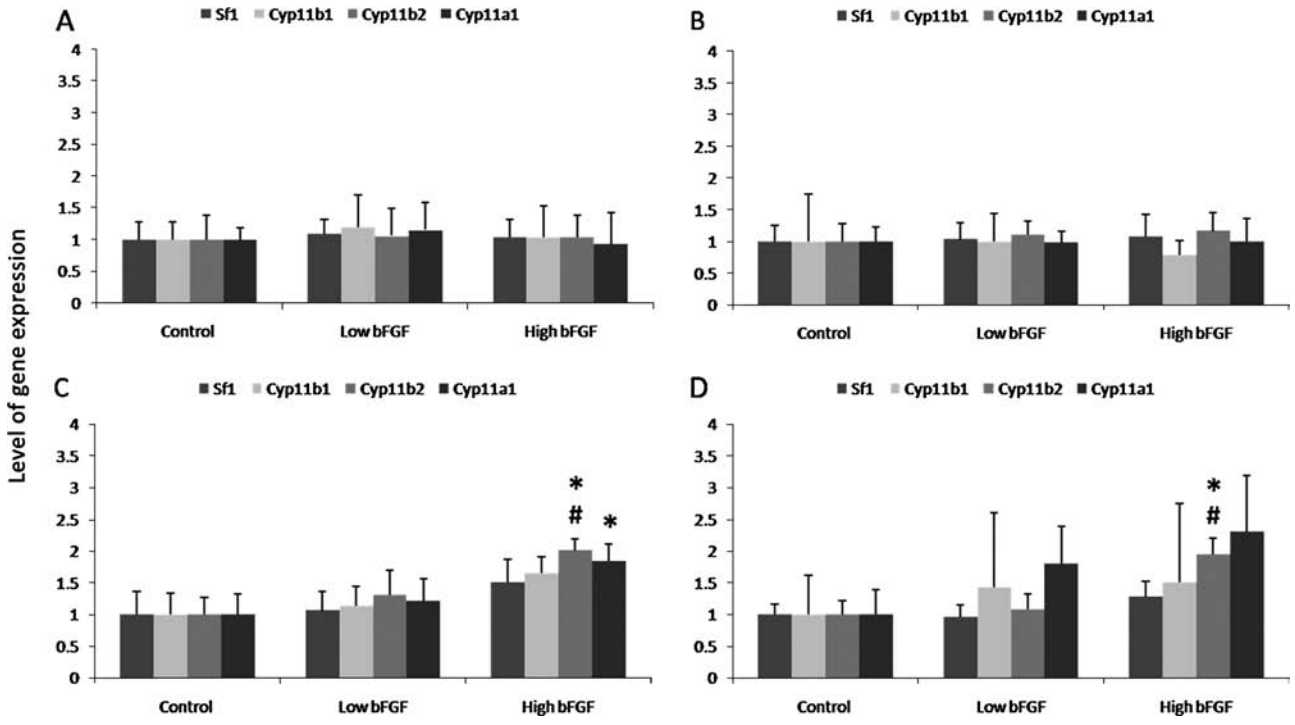

FIG. 8. Relative gene expression of adrenal cortical markers in retrieved implants. Implants were retrieved on days 10, 28, and 56. (**A**) Relative gene expression levels of cells before implantation. (**B–D**) Relative gene expression levels of implants on days 10, 28, and 56, respectively. The relative expression level of each adrenal-specific gene was normalized to that of the control group from the same time point. The gene expression of the high bFGF group was compared to that of the control and low bFGF groups. The gene expression of the low bFGF group was compared to that of the control group. $^{*}p < 0.05$ as compared to the control group, and $^{\#}p < 0.05$ as compared to the low bFGF group. Error bar represents standard deviation of measurements of retrieved implants from three animals.

number were not directly correlated with the dose of bFGF delivered. This correlation suggests that bFGF may directly or indirectly affect the tissue remodeling during the wound healing process. This may be due to the consequence of increased matrix metalloproteinases activities upregulated by bFGF that are capable of degrading of extracellular matrix proteins.[37,38] The decreased implant size may also be due to wound contraction. Studies have demonstrated that bFGF can stimulate wound contraction during a healing process. Genetic deletion of bFGF in mice leads to lack of wound contraction in the process of myocardial infarct repair,[39] and accelerates wound contraction after burn wounds in diabetic mice.[40] Another possible explanation is that the presence of glucocorticoid impairs collagen deposition. bFGF stimulation might have resulted in an elevated level of local glucocorticoid secretion. Previous studies showed that the treatment of cultured fibroblasts with dexamethasone, a potent synthetic glucocorticoid, decreases collagen synthesis, and thus glucocorticoids may directly decrease collagen deposition *in vivo*.[41,42] The smaller implant resulted in fewer cells present in the high bFGF group due to the physical limitation placed on the number of cells within the implant.

After 56 days, both bFGF groups had significantly higher implant weights and cell numbers than the control group. The large decrease in the size of the control group may be due to contraction and breakdown of the collagen sponge. Although both the low and high groups had larger implants than the control group on day 56, a drastic remodeling of the original implant was observed only in the high bFGF group, where the implants had a highly uniform distribution of blood vessels. While the increased cell mass from days 28 to 56 in the high bFGF group could be due to an increase in nonadrenal cell types, the increased expression of Sf1 implied that there was also an increase in the proportion of the adrenal cortical cells. Sf1 is a molecular identification of the adrenal cortical cell.[43] Expression of this nuclear receptor is a prerequisite for adrenal cortical formation and differentiation.[44] A decreased level of Sf1 expression from the initial implantation to day 28 suggests a decrease in the proportion of adrenal cortical cells. The increased level of Sf1 expression on day 56, along with the increased cell number, suggests adrenal cortical cell growth in the implants. On days 28 and 56, significantly higher levels of *Cyp11b2* and *Cyp11a1* expression were also found in the high bFGF group. *Cy11b2* and *Cy11a1* are both crucial to the production of aldosterone and are typically found in cells in the zona glomerulosa. Based on the results from low and high bFGF groups, the higher dose of bFGF may have upregulated the expression of these genes. However, future experiments with additional bFGF concentrations may be necessary to identify an optimal dose. Further, despite their statistical difference, less than two-fold increase in the high bFGF groups for *Cyp11b2* and *Cyp11a1* when compared to the control groups does not provide strong evidence for physiological significance. Whether or not bFGF is associated with the regulation of those specific genes is still questionable.

In conclusion, bFGF delivery increased the growth of adrenal cortical cells within the implants. The steroidogenic gene expression was not substantially altered by the delivery of bFGF. The delivery of bFGF may have increased the overall adrenal cortical function based on the increase in the number of adrenal cortical cells.

Acknowledgments

This work was funded by National Institutes of Health (DK068207) and Fubon Foundation.

Disclosure Statement

No competing financial interests exist.

References

1. Oelkers, W. Adrenal insufficiency. N Engl J Med **335,** 1206, 1996.
2. Jeffcoate, W. Assessment of corticosteroid replacement therapy in adults with adrenal insufficiency. Ann Clin Biochem **36,** 151, 1999.
3. Dunn, J.C., Chu, Y., Lam, M.M., Wu, B.M., Atkinson, J.B., and McCabe, E.R. Adrenal cortical cell transplantation. J Pediatr Surg **39,** 1856, 2004.
4. Mitani, F., Mukai, K., and Miyamoto, H. The undifferentiated cell zone is a stem cell zone in adult rat adrenal cortex. Biochem Biophys Acta **1619,** 317, 2003.
5. Esch, F., Baird, A., Ling, N., Ueno, N., Hill, F., Denoroy, L., Klepper, R., Gospodarowicz, D., Bohlen, P., and Guillemin, R. Primary structure of bovine pituitary basic fibroblast growth factor (FGF) and comparison with the amino-terminal sequence of bovine brain acidic FGF. Proc Natl Acad Sci USA **82,** 6507, 1985.
6. Schweigerer, L., Neufeld, G., Friedman, J., Abraham, J.A., Fiddes, J.C., and Gospodarowicz, D. Basic fibroblast growth factor: production and growth stimulation in cultured adrenal cortex cells. Endocrinology **120,** 796, 1987.
7. Savona, C., and Feige, J.J. cAMP-mediated regulation of adrenocortical cell bFGF receptors. Ann NY Acad Sci **638,** 412, 1991.
8. Mesiano, S., Mellon, S.H., Gospodarowicz, D., Di Blasio, A.M., and Jaffe, R.B. Basic fibroblast growth factor expression is regulated by corticotropin in the human fetal adrenal: a model for adrenal growth regulation. Proc Natl Acad Sci USA **88,** 5428, 1991.
9. Basile, D.P., and Holzwarth, M.A. Basic fibroblast growth factor receptor in the rat adrenal cortex: effects of suramin and unilateral adrenalectomy on receptor numbers. Endocrinology **134,** 2482, 1994.
10. Montesano, R., Vassalli, J.D., Baird, A., Guillemin, R., and Orci, L. Basic fibroblast growth factor induces angiogenesis *in vitro*. Proc Natl Acad Sci USA **83,** 7297, 1986.
11. Gospodarowicz, D., Cheng, J., and Lirette, M. Bovine brain and pituitary fibroblast growth factors: comparison of their abilities to support the proliferation of human and bovine vascular endothelial cells. J Cell Biol **97,** 1677, 1983.
12. Tsuboi, R., Sato, Y., and Rifkin, D.B. Correlation of cell migration, cell invasion, receptor number, proteinase production, and basic fibroblast growth factor levels in endothelial cells. J Cell Biol **110,** 511, 1990.
13. Pepper, M., Ferrara, N., Orci, L., and Montesano, R. Potent synergism between vascular endothelial growth factor and basic fibroblast growth factor in the induction of angiogenesis *in vitro*. Biochem Biophys Res Commun **189,** 824, 1992.
14. Mattern, J., Koomagi, R., and Volm, M. Coexpression of VEGF and bFGF in human epidermoid lung carcinoma is associated with increased vessel density. Anticancer Res **17,** 2249, 1997.
15. Stavri, G.T., Zachary, I.C., Baskerville, P.A., Martin, J.F., and Erusalimsky, J.D. Basic fibroblast growth factor upregulates

the expression of vascular endothelial growth factor in vascular smooth muscle cells. Synergistic interaction with hypoxia. Circulation **92,** 11, 1995.
16. Kushibiki, T., and Tabata, Y. A new gene delivery system based on controlled release technology. Curr Drug Deliv **1,** 153, 2004.
17. Lu, Y. Recombinant adeno-associated virus as delivery vector for gene therapy: a review. Stem Cells Dev **13,** 133, 2004.
18. Thomas, M., Northrup, S.R., and Hornsby, P.J. Adrenocortical tissue formed by transplantation of normal clones of bovine adrenocortical cells in acid mice replaces the essential functions of the animals' adrenal glands. Nat Med **3,** 978, 1997.
19. Rinsch, C., Quinodoz, P., Pittet, B., Alizadeh, N., Baetens, D., Montandon, D., Aebischer, P., and Pepper, M.S. Delivery of FGF-2 but not VEGF by encapsulated genetically engineered myoblasts improves survival and vascularization in a model of acute skin flap ischemia. Gene Ther **8,** 523, 2001.
20. Lee, K.Y., Peters, M.C., and Mooney, D.J. Comparison of vascular endothelial growth factor and basic fibroblast growth factor on angiogenesis in SCID mice. J Control Rel **87,** 49, 2003.
21. Lee, M., Wu, B.M., Stelzner, M., Reichardt, H.M., and Dunn, J.C. Intestinal smooth muscle cell maintenance by basic fibroblast growth factor. Tissue Eng **14,** 1395, 2008.
22. Lee, M., Chen, T.T., Iruela-Arispe, M.L., Wu, B.M., and Dunn, J.C. Modulation of protein delivery from modular polymer scaffolds. Biomaterials **28,** 1862, 2007.
23. Mooney, D.J., Organ, G., Vacanti, J.P., and Langer, R. Design and fabrication of biodegradable polymer devices to engineer tubular tissues. Cell Transpl **3,** 203, 1994.
24. Lavik, E., and Langer, R. Tissue engineering: current state and perspectives. Appl Microbiol Biotechnol **65,** 1, 2004.
25. Anderson, J.M., and Shive, M.S. Biodegradation and biocompatibility of PLA and PLGA microspheres. Adv Drug Deliv Rev **28,** 5, 1997.
26. Eldridge, J.H., Staas, J.K., Tice, T.R., and Gilley, R.M. Biodegradable poly(DL-lactide-*co*-glycolide) microspheres. Res Immunol **143,** 557, 1992.
27. Lee, M., Chen, T.T., Iruela-Arispe, M.L., Wu, B.M., and Dunn, J.C.Y. Modulation of protein delivery from modular polymer scaffolds. Biomaterials **28,** 1862, 2007.
28. Chu, Y., Wu, B.M., McCabe, E.R., and Dunn, J.C. Serum-free cultures of murine adrenal cortical cells. J Pediatr Surg **41,** 2008, 2006.
29. Yang, L.V., Radu, C.G., Roy, M., Lee, S., McLaughlin, J., Teitell, M.A., Iruela-Arispe, M.L., and Witte, O.N. Vascular abnormalities in mice deficient for the G protein-coupled receptor GPR4 that functions as a pH sensor. Mol Cell Biol **27,** 1334, 2007.
30. Jilani, S.M., Murphy, T.J., Thai, S.N.M., Eichmann, A., Alva, J.A., and Iruela-Arispe, M.L. Selective binding of lectins to embryonic chicken vasculature. J Histochem Cytochem **51,** 597, 2003.
31. Lee, S., Jilani, S.M., Nikolova, G.V., Carpizo, D., and Iruela-Arispe, M.L. Processing of VEGF-A by matrix metalloproteinases regulates bioavailability and vascular patterning in tumors. J Cell Biol **169,** 681, 2005.
32. Chung, H.J., Kim, H.K., Yoon, J.J., and Park, T.G. Heparin immobilized porous PLGA microspheres for angiogenic growth factor delivery. Pharm Res **23,** 1835, 2006.
33. Ahrendt, G., Chickering, D.E., and Ranieri, J.P. Angiogenic growth factors: a review for tissue engineering. Tissue Eng **4,** 117, 1998.
34. Basile, D.P., and Holzwarth, M.A. Basic fibroblast growth factor may mediate proliferation in the compensatory adrenal growth response. Am J Physiol Regul Integr Comp Physiol **265,** R1253, 1993.
35. Hornsby, P.J. Transplantation of adrenocortical cells. Rev Endocr Metab Disord **2,** 313, 2001.
36. Thomas, M., and Hornsby, P.J. Transplantation of primary bovine adrenocortical cells into acid mice. Mol Cell Endocrinol **153,** 125, 1999.
37. Krishnan, L., Hoying, J.B., Nguyen, H., Song, H., and Weiss, J.A. Interaction of angiogenic microvessels with the extracellular matrix. Am J Physiol Heart Circ Physiol **293,** H3650, 2007.
38. Xie, J., Bian, H., Qi, S., Xu, Y., Tang, J., Li, T., and Liu, X. Effects of basic fibroblast growth factor on the expression of extracellular matrix and matrix metalloproteinase-1 in wound healing. Clin Exp Dermatol **33,** 176, 2008.
39. Jitka, A.I., Virag, M.L.R., Reece, J., Hardouin, S., Feigl, E.O., and Murry, C.E. Fibroblast growth factor-2 regulates myocardial infarct repair. Am J Pathol **171,** 1431, 2007.
40. Okumura, M.O.T., Nakamura, T., and Yajima, M. Effect of basic fibroblast growth factor on wound healing in healing-impaired animal models. Arzneimittelforschung **46,** 547, 1996.
41. Slavin, J., Unemori, E., Hunt, T.K., and Amento, E. Transforming growth factor beta (TGF-beta) and dexamethasone have direct opposing effects on collagen metabolism in low passage human dermal fibroblasts *in vitro*. Growth Fact **11,** 205, 1994.
42. Slavin, J. The role of cytokines in wound healing. J Pathol **178,** 5, 1996.
43. Kim, A.C., and Hammer, G.D. Adrenocortical cells with stem/progenitor cell properties: recent advances. Mol Cell Endocrinol **265–266,** 10, 2007.
44. Luo, X., Ikeda, Y., and Parker, K.L. A cell-specific nuclear receptor is essential for adrenal and gonadal development and sexual differentiation. Cell **77,** 481, 1994.

Address correspondence to:
James C.Y. Dunn, M.D., Ph.D.
Biomedical Engineering Interdepartmental Program
Department of Bioengineering
University of California
MC 709818, 10833 Le Conte Ave.
Los Angeles, CA 90095-7098

E-mail: jdunn@mednet.ucla.edu

Received: May 26, 2008
Accepted: December 5, 2008
Online Publication Date: January 19, 2009